24th INTERNATIONAL CONGRESS ON SOUND AND VIBRATION
23–27 July 2017, London

ICSV24
23-27JULY 2017
LONDON CALLING

DEVELOPMENT AND APPLICATION OF OPTIMISED COMPACT DIFFERENCE SCHEMES TO LINEAR ACOUSTICS PROBLEMS IN ORTHOGONAL CURVILINEAR COORDINATES

Christopher Beckwith
University of Greenwich, London, UK
email: C.J.Beckwith@greenwich.ac.uk

Koulis Pericleous
University of Greenwich, London, UK

Valdis Bojarevics
University of Greenwich, London, UK

Two families of optimised compact difference schemes are presented. The first uses Holberg's minimised Group Velocity (MGV) approach, and the second uses an approach based on previous development of Dispersion Relation Preserving (DRP) schemes on vertex based grids. The resulting schemes are compared analytically and experimentally to previously published MGV and DRP optimised schemes. The new schemes are shown to have reduced phase velocity errors, and greater resolving efficiency. Some simple benchmark problems are solved with the obtained schemes using Linearized Euler Equations without convective terms, before being extended to orthogonal curvilinear coordinate systems and applied to 2-dimensional wave problems. The extension is simplified to minimise the need to interpolate derivatives at undefined locations, and allows for the efficient and accurate handling of complex material boundaries.

Keywords: Compact Difference, Staggered, Curvilinear, Acoustics

1. Introduction

Optimised Finite Difference schemes have been commonplace in the computational simulation of various wave propagation problems. Implicit Compact Difference schemes largely act as an extension of these, but are able to obtain much greater levels of accuracy while using the same stencil size of an equivalent Explicit Finite Difference scheme.

Since their introduction, a number of authors including Kim and Lee (1996), Kim (2007), and Liu et al. (2008) have attempted to optimise the standard compact FD scheme by extending the DRP approach developed by Tam and Webb (1993). The vast majority of these efforts have been on the vertex based approach, despite the fact that staggered schemes have been shown to exhibit less dispersive behaviour than their vertex based counterparts. Recently, Venutelli (2011) has attempted to use Holberg's MGV approach on staggered grids and obtained promising results, but the potential for modified versions of MGV, or the application of existing DRP techniques, to staggered compact difference schemes is an area that is still unexplored. This represents the first motivation of this work. The second motivation of this work is comes from their practical usage, as a number of complications can arise from the use of staggered compact difference schemes. These include implementation difficulties on complex-shape domains and the additional computation needed to interpolate midpoint

values of decision variables. A curvilinear scheme, which is based on a reduced form of the Linearized Euler equations and solved in a Leapfrog type manner, is presented which aims to minimise these problems.

2. Optimised Schemes

The standard staggered compact difference scheme for a first derivative Lele(1992), on a six-point stencil takes the form:

$$\beta f'_{i-2} + \alpha f'_{i-1} + f'_i + \alpha f'_{i+1} + \beta f'_{i+2} = a\frac{f_{i+\frac{1}{2}} - f_{i-\frac{1}{2}}}{h} + b\frac{f_{i+\frac{3}{2}} - f_{i-\frac{3}{2}}}{3h} + c\frac{f_{i+\frac{5}{2}} - f_{i-\frac{5}{2}}}{5h} \tag{1}$$

The terms α, β, a, b and c can be obtained by solving the following relations, up to a chosen order of accuracy:

2nd order:

$$a + b + c = 2\beta + 2\alpha + 1 \tag{2}$$

4th order:

$$(\frac{1}{2})^2 a + (\frac{3}{2})^2 b + (\frac{5}{2})^2 c = 3!(\alpha + 2^2\beta) \tag{3}$$

6th order:

$$(\frac{1}{2})^4 a + (\frac{3}{2})^4 b + (\frac{5}{2})^4 c = 2\frac{5!}{4!}(\alpha + 2^4\beta) \tag{4}$$

8th order:

$$(\frac{1}{2})^6 a + (\frac{3}{2})^6 b + (\frac{5}{2})^6 c = 2\frac{7!}{6!}(\alpha + 2^6\beta) \tag{5}$$

10th order:

$$(\frac{1}{2})^8 a + (\frac{3}{2})^8 b + (\frac{5}{2})^8 c = 2\frac{9!}{8!}(\alpha + 2^8\beta) \tag{6}$$

If all equations are solved simultaneously, a single 10th order scheme is obtained (Lele, 1992). However optimised schemes can be obtained by reducing the order of accuracy and substituting the unwanted equations in the system for alternative equations. This forms the basis of both the MGV approach (Holberg, 1987) and the DRP approach. To begin, first it is important to transform the compact scheme (1) into the wavenumber domain using a Fourier transform.

$$\bar{k} = \frac{(2a)sin(\frac{1}{2}k) + (\frac{2}{3}b)sin(\frac{3}{2}k) + (\frac{2}{5}c)sin(\frac{5}{2}k)}{1 + 2\alpha cos(k) + 2\beta cos(2k)} \tag{7}$$

All following schemes use different strategies of optimising the compact difference parameters in this wavenumber domain. The schemes compared are Venutelli (2011), and two new schemes introduced in this paper. The first is a 2 parameter extension of his MGV approach, which begins with the definition of the integrated error function E:

$$E = \int_0^r (\frac{d\bar{k}}{dk} - 1)^2[(1 + \alpha cos(k) + 2\beta cos(2k))^4(\frac{k}{r})^n dk \tag{8}$$

The optimal values of r and n can then be found for schemes of 8th or lower order accuracy. For example, for a 6th order scheme, equations (2)-(4) are used, with 2 additional constraints to make the solution well defined:

$$\frac{\partial E}{\partial \alpha} = \frac{\partial E}{\partial \beta} = 0 \tag{9}$$

$$\frac{d\bar{k}}{dk} - 1 \leq \gamma \quad \forall \quad 0 \leq k \leq r \tag{10}$$

Where γ represents an acceptable tolerance level. A value of $\gamma = 0.01$ is taken to match that used by Venutelli. The task is then to maximise r.

The second approach is analogous to Kim (2007)'s method for non-staggered grids. The integrated error function for this scheme takes the form:

$$E = \int_0^r (\bar{k} - k)^2 [(1 + \alpha cos(k) + 2\beta cos(2k))^2 (\frac{k}{r})^n dk \tag{11}$$

The optimisation procedure is functionally identical to that of existing DRP based methods. While a number of optimisation strategies could be used, the one used in this paper is a Maple implementation of the Conjugate Direction with Orthogonal Shift (CDOS) method developed by Moiseev (2011). This method has been shown to be effective at handling problems of a highly non-linear nature. A tolerance level of 0.0001 is used, matching that of previous studies on vertex based methods. The results in Table 2 show significantly greater resolution than Kim, who achieved $k_c = 0.839\pi$ at 4^{th} order accuracy, where k_c represents the lowest value for which the relative error of the computed wavenumber falls outside a tolerance level when compared to the real wavenumber. For this paper, a tolerance of 0.001 is used to match that of previous work.

Table 1: Obtained schemes with the modified MGV approach

Scheme	n	r	a	b	c	α	β
4^{th} order	22	$.866\pi$	.5501888045	1.412144220	.1944680976	.5195175641	.0588829967
6^{th} order	22	$.822\pi$	.6248746793	1.265245254	.1115338503	.4622076859	.0386192058
8^{th} order	22	$.753\pi$	.7147338451	1.0614935332	.0643347795	.3954227561	.0248583228

Table 2: Obtained schemes with the modified DRP approach

Scheme	n	k_c	a	b	c	α	β
6^{th} order	11	$.875\pi$	.6295951077	1.2560279016	.1077103518	.4590749488	.0375917317
8^{th} order	12	$.788\pi$	.7215710857	1.0444900869	.0621004685	.3899620161	.0241188040

3. Comparison of Schemes

Once the coefficients are obtained, we can determine the resolution and phase speed characteristics of the schemes. The MGV schemes are compared with those obtained by Venutelli(2011), while the DRP Schemes are only compared with Lele's original unoptimised scheme due to the lack of research into this family. In Figure 1, we see that both approaches yield less dispersive schemes than the unoptimised 10th order scheme, but the MGV schemes tend to overshoot, which causes greater dispersive error at certain wavenumbers. The 6th order DRP scheme stays within the tolerance level of 0.1% for the largest range of wavenumbers.

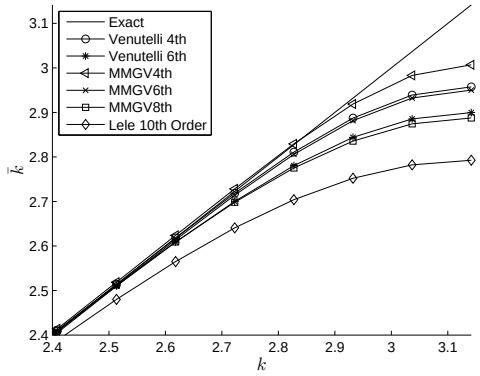

(a) MGV optimised schemes show less dispersive behaviour than the unoptimised scheme. However, the 4th order scheme overshoots at lower wavenumbers.

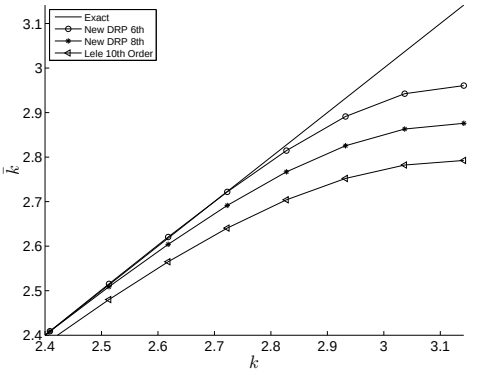

(b) Schemes optimised with the DRP approach show similar behaviour to their MGV counterparts, but do not overshoot at lower wavenumbers.

Figure 1: Modified Wavenumber vs Wavenumber plots for both families of optimised schemes, zoomed in to focus on higher wavenumbers.

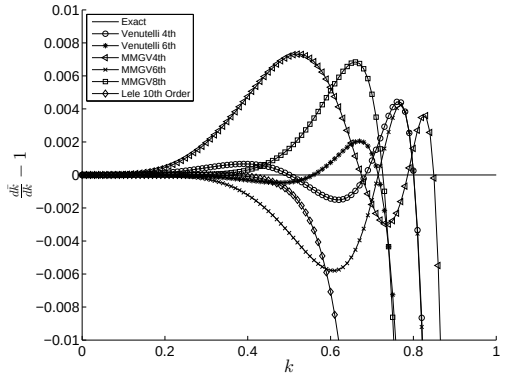

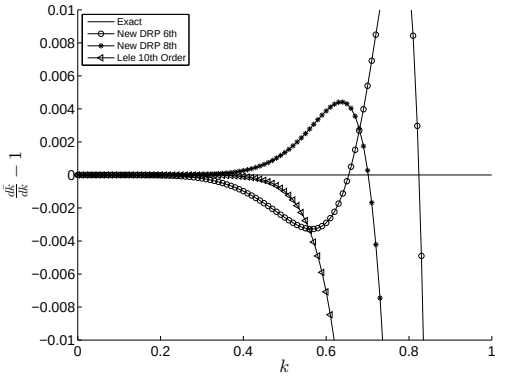

Figure 2: Group velocity plots for MGV schemes (left) and DRP schemes (right), compared to the exact solution and the unoptimised scheme.

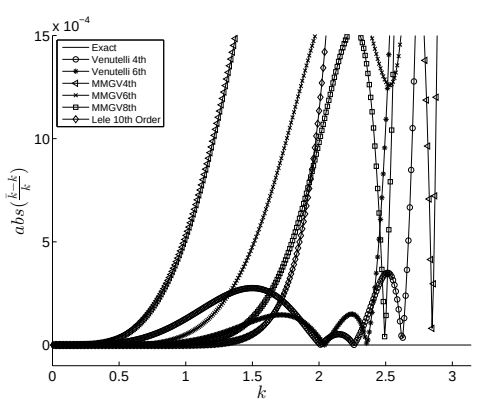

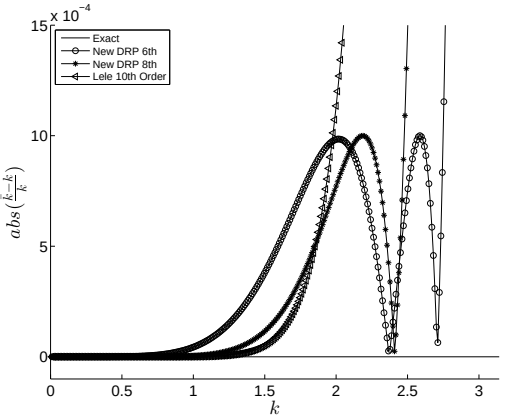

Figure 3: Resolution error for the MGV schemes (left) and DRP schemes (right), compared to the exact solution and the unoptimised scheme.

In Figure 2, we see that the modifications to the MGV approach allow the scheme to fluctuate more at lower range numbers, under the condition that their error stays within the tolerance of 1%. This is is what causes the overshooting errors that we see in Figure 1. Meanwhile, in Figure 3 we see

the resolution error. This is a useful way of visualising the deviation in Figure 1, and shows the the relative error

4. Benchmark Problem

To compare and validate the accuracy of the schemes in real world simulations, a model is implemented with a simplified version of the Linearized Euler Equations. All convective terms are ignored, and the following equations are obtained for a general number of dimensions, j:

$$\frac{\partial p}{\partial t} = -\bar{\rho}c^2 \frac{\partial v_j}{\partial x_j} \tag{12}$$

$$\frac{\partial v_j}{\partial t} = -\frac{1}{\bar{\rho}} \frac{\partial p}{\partial x_j} + F \tag{13}$$

Where F is an additional source term. A 1D model of these simplified equations are then solved in a Leapfrog-esque manner. This staggering allows the cell centred schemes to be used without midpoint interpolation. Using this formulation, a benchmark problem is set up which is similar to that in Tam (1995). A theoretical fluid is used with $\rho = c = 1$, and run on a domain with $-20 < x < 450$. An initial velocity is set to:

$$u = 0.5exp\left(- ln(2)(\frac{x}{5})^2 \right) \tag{14}$$

The simulation is run with two different values $\Delta x = 2$ and $\Delta x = 3.55$, to demonstrate how the schemes perform at different points per wavelength. For agreement with the benchmark problem, the simulation is run up until $t = 400$ and then compared with the exact solution. The L_2-norm is taken for each scheme at the end of the simulation and compared in Tables 3 and 4.

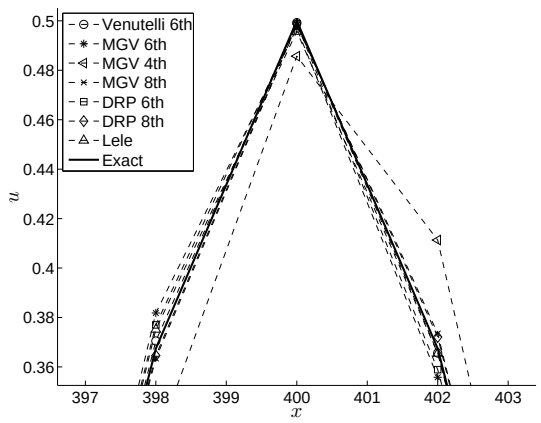

(a) Using $\Delta x = 2$, most schemes have a good agreement with the exact solution.

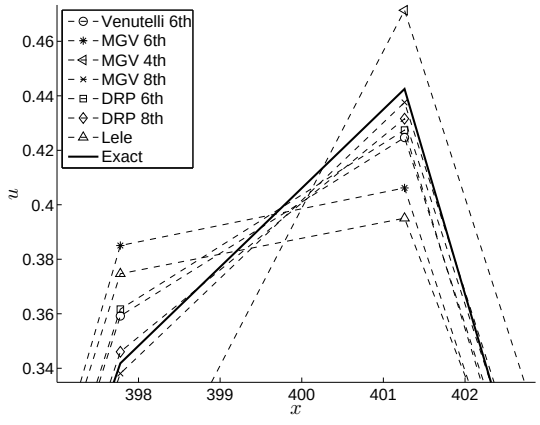

(b) At $\Delta x = 3.55$, the 6^{th} order DRP scheme and Venutelli's scheme produce the best results, but all schemes struggle.

Figure 4: Zoomed in waveforms at t=400, comparisons made between Venutelli's 6th order scheme, Lele's unoptimised scheme, and the proposed schemes.

At $\Delta x = 2$ we see that all schemes achieve great results. This is not surprising as all of the optimised schemes with the exception of the 4^{th} order MGV scheme have extremely high accuracy at lower wavenumbers. At $\Delta x = 3.55$ the schemes are tested much more, and some schemes like the 4^{th} order MGV perform rather poorly, while our 6^{th} order DRP actually performs better than Venutelli's, and significantly better than the unoptimised scheme.

Table 3: L_2-norm at $\Delta x = 2$

Scheme	L_2-norm
Venutelli 6^{th}	0.0046
Modified MGV 4^{th}	0.0704
Modified MGV 6^{th}	0.0218
Modified MGV 8^{th}	0.0105
Modified DRP 6^{th}	0.0157
Modified DRP 8^{th}	0.0083
Lele 10^{th}	0.0145

Table 4: L_2-norm at $\Delta x = 3.55$

Scheme	L_2-norm
Venutelli 6^{th}	0.0405
Modified MGV 4^{th}	0.1166
Modified MGV 6^{th}	0.0628
Modified MGV 8^{th}	0.0475
Modified DRP 6^{th}	0.0404
Modified DRP 8^{th}	0.0485
Lele 10^{th}	0.0984

5. Curvilinear Coordinates

It has been shown by Tam (2012) that a numerical scheme that has been optimised to have DRP properties, will maintain those properties when used in curvilinear coordinates as long as the grid meets some certain criteria. It can also be shown that an MGV optimised scheme can also be used under similar conditions. To enable the use of staggered grids with the curvilinear transformed version of equations (12)-(13), a form must be derived with minimal use of cross derivatives which are not defined in the cell centres. This is done by using a similar derivation to the one used by Xie et al. (2002) for solving Maxwell's equations. In 2D, the obtained equations have the form:

$$\frac{\partial \phi^{\xi}}{\partial t} = \frac{1}{\rho J^2}\frac{\partial p}{\partial \xi}(-y_{\eta}^2 - x_{\eta}^2) \tag{15}$$

$$\frac{\partial \phi^{\eta}}{\partial t} = \frac{1}{\rho J^2}\frac{\partial p}{\partial \eta}(-y_{\xi}^2 - x_{\xi}^2) \tag{16}$$

$$\frac{\partial p}{\partial t} = -\rho c^2\left(\frac{\partial \phi^{\xi}}{\partial \xi} + \frac{\partial \phi^{\eta}}{\partial \eta} + Q\phi^{\xi} + R\phi^{\eta}\right) + F \tag{17}$$

$$Q = \frac{1}{J}(y_{\eta}x_{\xi\xi} - y_{\xi}x_{\xi\eta} - x_{\eta}y_{\xi\xi} + x_{\xi}y_{\xi\eta}) \tag{18}$$

$$R = \frac{1}{J}(y_{\eta}x_{\eta\xi} - y_{\xi}x_{\eta\eta} - x_{\eta}y_{\eta\xi} + x_{\xi}y_{\eta\eta}) \tag{19}$$

Where $J = x_{\xi}y_{\eta} - y_{\xi}x_{\eta}$ is the determinant of the Jacobian. A 3D extension, or one containing additional terms is also possible. These equations are only valid when solved on orthogonal domains, so it is important that the grid generation procedure produces orthogonal grids. This is not a significant restriction as orthogonality is often desirable, since this often leads to significant simplification of both the transformed equations and the application of boundary conditions. Orthogonal schemes also do not suffer from the numerical instabilities that can arise from cell deformity on non-orthogonal grids. However, since the value of ϕ^{ξ} and ϕ^{η} are not defined at the stored pressure locations, some midpoint interpolation is still required, which is handled with the standard 10th order compact scheme:

$$\beta\hat{f}_{i-2} + \alpha\hat{f}_{i-1} + \hat{f}_i + \alpha\hat{f}_{i+1} + \beta\hat{f}_{i+2} = a\frac{f_{i+\frac{1}{2}} + f_{i-\frac{1}{2}}}{2} + b\frac{f_{i+\frac{3}{2}} + f_{i-\frac{3}{2}}}{2} + c\frac{f_{i+\frac{5}{2}} + f_{i-\frac{5}{2}}}{2} \tag{20}$$

With $\alpha = \frac{10}{21}$, $\beta = \frac{5}{126}$, $a = \frac{5}{3}$, $b = \frac{5}{14}$, $c = \frac{1}{126}$. This can be optimised, but additional work needs to be done to obtain the best possible scheme.

5.1 Results

An initial validation is performed on a simple resonating disk with a diameter of $0.4m$. A theoretical fluid is used with $\rho = 999kg/m^3$ and $c = 2500m/s$, and is vibrated at its forcing frequency. The

frequency is obtained using an Eigenfrequency study with PARDISO solvers within COMSOL Multiphysics, and is calculated to be approximately $7623Hz$. This is then used in a time dependent study using the newly obtained transformed equations, with derivatives calculated using the new 8th order DRP scheme. To ensure grid orthogonality, and to remove the dependence on grid generation, traditional polar coordinates are used. In the θ direction, a periodic boundary condition is implemented, while in the radial direction, the outside edge of the disk is assumed to have zero normal velocity, $\phi^r = 0$. For stability and simplicity, this is implemented with a symmetry boundary condition.

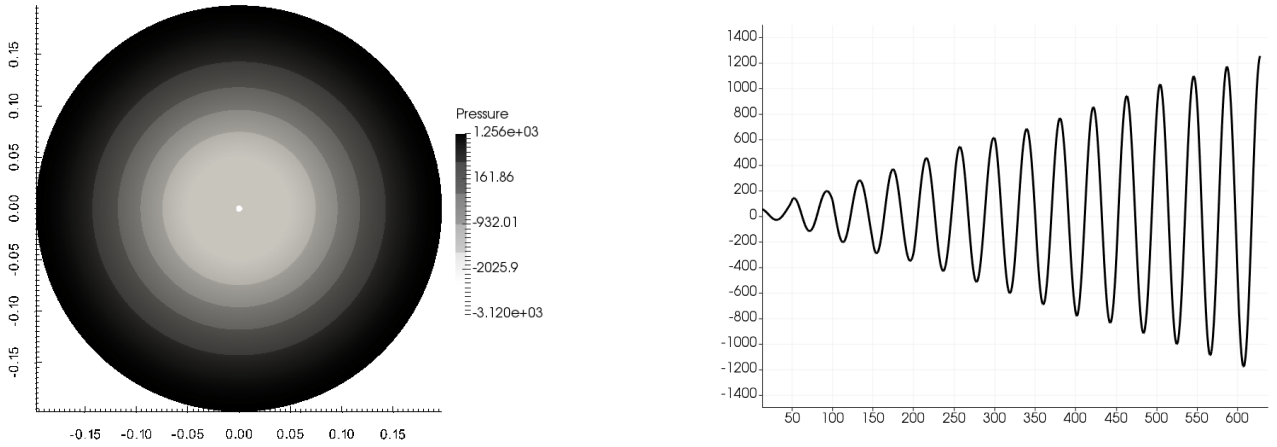

Figure 5: Resonant mode calculated with the compact scheme (left) at 7623Hz agrees with the COMSOL study. Time dependant pressure at a node on the outside edge of the disk (right) shows the expected linearly increasing peak pressure.

A second validation is performed to test the schemes on a grid that has been generated using the CRDT algorithm (Driscoll, 1998), and demonstrates a potential application for measuring acoustic pressure inside a crucible with a vibrating top surface. The crucible is filled with Aluminium and is excited with the aid of an electromagnetic coil above the top surface. An oxide layer develops on the top of the fluid and in the model is approximated as a reflecting solid wall. Material properties have been approximated to be $\rho = 2375kg/m^3$ and $c = 4600m/s$.

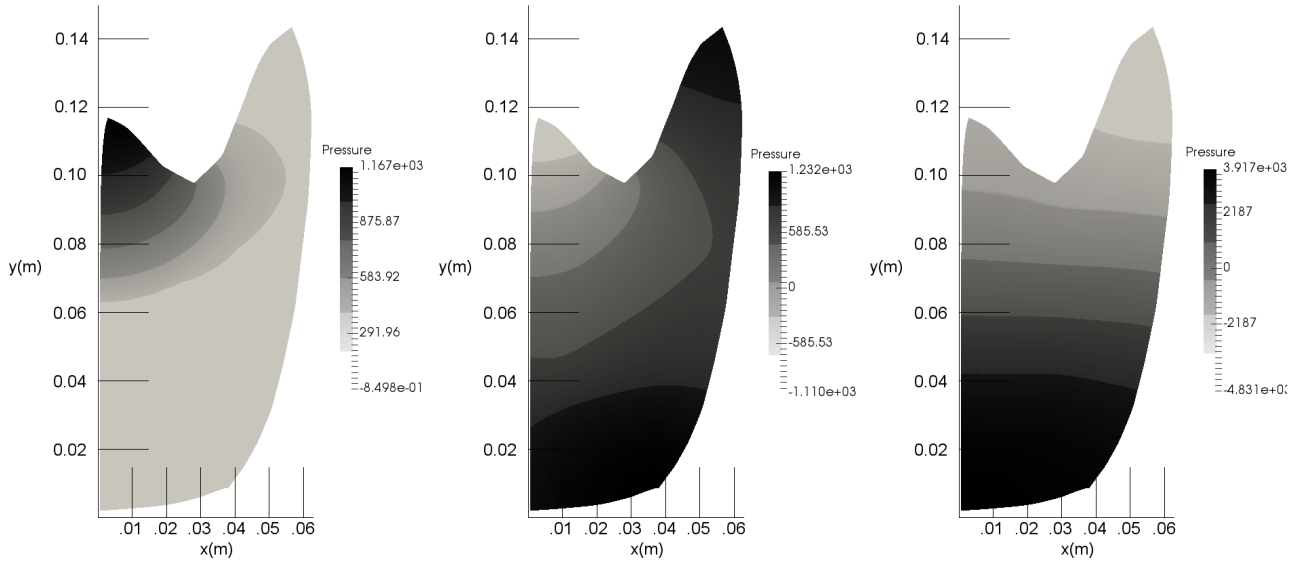

(a) $t \approx 5.5 \times 10^{-6}s$ (b) $t \approx 1.6 \times 10^{-5}s$ (c) $t \approx 7.6 \times 10^{-4}s$

Figure 6: Pressure distributions in the crucible at 3 timesteps - Soon after the electromagnetic field is activated (a), when the waves start reflecting (b), and some time later when the crucible is resonating (c)

An eigenfrequency study performed in COMSOL resulted in a fundamental frequency of $17906Hz$, which is then used as part of a time dependant study using the newly obtained 8th order DRP scheme. Snapshots at 3 different timesteps are shown in Figure 6. As before, the simulation agrees with the COMSOL study as resonance is achieved.

6. Conclusions and Future Work

Two new families of staggered Compact Finite Difference schemes have been presented, with some simple test cases demonstrating their use. The schemes optimised with the DRP based techniques has led to new schemes with significantly better resolution properties than their vertex based counterparts, and compare well to the MGV optimised staggered scheme proposed by Venutelli(2011). However, attempts to modify the MGV approach with similar techniques were only partially successful. In addition, when used with the newly obtained transformed equations (15)-(19), excellent accuracy is achieved on domains with complex shapes. However, the current method is limited only to 2D domains, and a formulation does not yet exist for use with 3D cases. Development of such equations is an important step for some realistic applications, and is part of continued study.

REFERENCES

1. Lele, S.K, Compact finite difference schemes with spectral-like resolution, *Journal of Computational Physics*, **103**, 16–42, (1992).
2. Kim, J.W and Lee, D.J, optimised Compact Finite Difference Schemes with Maximum Resolution, *AIAA JOURNAL*, (1996)
3. Kim, J.W,Optimised boundary compact finite difference schemes for computational aeroacoustics, *Journal of Computational Physics*, **225**, 995–1019, (2007).
4. Liu, Z., Huang, Q., Zhao, Z. and Yuan, J., optimised Compact Finite Difference Schemes with High Accuracy and Maximum Resolution, *International Journal of Aeroacoustics*, **7**, 123–146 , (2008).
5. Tam, C.K.W., Webb, J.C., Dispersion-Relation-Preserving Finite Difference Schemes for Computational Acoustics, *Journal of Computational Physics*, **107**, 262–281, (1993).
6. Tam, C.K.W., Webb, J.C., Dispersion-Relation-Preserving Finite Difference Schemes for Computational Acoustics, *Journal of Computational Physics*, **107**, 262–281, (1993).
7. Holberg, O., Computational aspects of the choice of operator and sampling interval for numerical differentiation in large-scale simulation of wave phenomena. *Geophysical Prospecting*, **35**, 629–655, (1987)
8. Tam, C.K.W., et al., Solutions of the benchmark problems by the dispersion-relation-preserving scheme, *NASA CONFERENCE PUBLICATION*, 1995.
9. Tam, C.K.W., Computational Aeroacoustics: A Wave Number Approach, *Cambridge Aerospace Series* **33**, Cambridge University Press, New York, (2012)
10. Xie, Z., Chan, C., Zhang, B., An Explicit Fourth-Order Orthogonal Curvilinear Staggered-Grid FDTD Method for Maxwell's Equation, *Journal of Computational Physics*, **175**, 739–763, (2002).
11. Venutelli, M., Holberg's optimisation for high-order compact finite difference staggered schemes, *International Journal of Computational Fluid Dynamics*, **25**, 287–296, (2011).
12. Moiseev, S.N., *Universal derivative-free optimisation method with quadratic convergence*, Kodofon, Russia, (2011), http://arxiv.org/abs/1102.1347.
13. Driscoll, T.A., and Vavasis, S.A., Numerical Conformal Mapping Using Cross-Ratios and Delaunay Triangulation, *SIAM J. SCI. COMPUT.*, **19**, 1783–1803, (1998)